

**An Improved Form for the Electrostatic Interactions  
of Polyelectrolytes in Solution and its  
Implications for the Analysis of QELSS Experiments  
on Sodium Dodecyl Sulfate and  
Cetyl Trimethyl Ammonium Bromide Solutions**

by

**Nicholas V. Sushkin**

ISBN: 1-58112-008-7

**DISSERTATION.COM**



1997

AN IMPROVED FORM FOR THE ELECTROSTATIC  
INTERACTIONS OF POLYELECTROLYTES IN SOLUTION AND  
ITS IMPLICATIONS FOR THE ANALYSIS OF QELSS  
EXPERIMENTS ON SODIUM DODECYL SULFATE AND CETYL  
TRIMETHYL AMMONIUM BROMIDE SOLUTIONS

by

Nicholas Sushkin

A Dissertation

Submitted to the faculty

of the

WORCESTER POLYTECHNIC INSTITUTE

in partial fulfillment of the requirements for the

Degree of Doctor of Philosophy

in

Physics

by

*Nicholas V. Sushkin*

August 1997

APPROVED:

*George D. J. Phillis*  
\_\_\_\_\_  
Professor George D. J. Phillis, Thesis Advisor

*L. R. Ram-Mohan*  
\_\_\_\_\_  
Professor L. R. Ram-Mohan, Committee Member

*Harvey Gould*  
\_\_\_\_\_  
Professor Harvey Gould, Clark University, Committee Member

## ABSTRACT

The electrostatic interaction between two charged spheres in the presence of a screening electrolyte is calculated at the level of the linearized Debye–Hückel theory. The calculation is performed analytically as a multipole expansion by applying two-center spherical harmonic expansions and symbolic manipulation methods. I focus on charge–charge and charge–induced dipole interactions, calculated for two spheres of possibly unequal size. The former interaction is given to good approximation by the familiar Debye–Hückel form  $\sim q_1 q_2 \exp[-\kappa(R - 2a)]/[\epsilon r(1 + \kappa a)^2]$ . The new results are the charge–induced dipole interactions. Physically, these terms arise from two sources: (i) surface polarization charge at the surface of each sphere, and (ii) exclusion of the counterion cloud of each sphere from the volume occupied by the other sphere. With parameters appropriate for micelles, the charge–induced dipole interactions dominate the charge–charge interaction at small separations.

Quasi-elastic light scattering measurements of the diffusion of sodium dodecyl sulfate (SDS) and cetyl trimethyl ammonium bromide (CTAB) micelles in aqueous solutions, and the diffusion of mesoscopic optical probes through the same solutions, were carried out at 35 °C and multiple solvent ionic strengths. Assuming a spherical micelle, I deduced the micelle radius, aggregation number, charge, and hydration from nonlinear least-squares fits to both probe and mutual diffusion data. For SDS micelles the charge that I find is lower than reported in the literature [Hayter, J. B.;

Penfold, J. *Colloid & Polymer Science* **1983**, *261*, 1022; Triolo, R.; Caponetti, E.; Graziano, V. *J. Phys. Chem.* **1985**, *89*, 5743. ] because I used an improved functional form of the micellar electrostatic interaction. I find a smaller aggregation number and a larger micellar hydration than literature values. My analysis of CTAB data implies extensive micellar growth, and failure of the spherical micelle assumption.

## ACKNOWLEDGMENTS

I would like to thank my advisor, Professor George D. J. Phillies, for his patient guidance and constant encouragement through all my years of study and research at WPI. From him I learned a lot of experimental and theoretical physics, technical writing, and the meaning of hard work. The support of a part of this work by the NSF under grant CHE91-15637 is gratefully acknowledged.

I would like to thank the Department of Physics, and particularly its Department Heads, Professors Stephen Jasperson and Thomas Keil, for providing me with financial assistantship. The department's support allowed me to conduct research and enjoy decent living conditions in the United States. I am grateful to Professors L. R. Ram-Mohan and Harvey Gould for serving on my thesis committee.

Roger Steele and Severin Ritchie provided valuable technical assistance. I thank them for contributing their time, skill, and smile to my experiments. Department secretaries Jean Flynn, Earline Rich, and Sue Milkman made sure that everything ran smoothly.

## CONTENTS

<i>Contents</i> . . . . .	v
<i>List of Figures</i> . . . . .	ix
<i>List of Tables</i> . . . . .	xi
<i>1. General Introduction</i> . . . . .	1
<i>2. Interaction of Polyelectrolytes</i> . . . . .	7
2.1 Introduction . . . . .	7
2.2 Historical . . . . .	8
2.3 Electrostatic Interactions — General Results . . . . .	15
2.4 Electrostatic Interactions – Closed Forms via Truncation . . . . .	31
2.5 Numerical Results for Micelles . . . . .	36
2.6 Discussion . . . . .	48
2.7 Conclusions . . . . .	54
<i>3. Microscopic parameters of CTAB and SDS Micelles</i> . . . . .	58
3.1 Introduction . . . . .	58
3.2 Historical . . . . .	61
3.3 Technique . . . . .	73

---

3.4	Experiment . . . . .	78
3.5	Experimental Results . . . . .	81
3.6	Theory . . . . .	85
3.7	Analysis . . . . .	92
3.8	Discussion . . . . .	97
3.9	Conclusions . . . . .	104
4.	<i>General Conclusions</i> . . . . .	111
	<i>Appendix</i>	113

## LIST OF FIGURES

1.1	Bond structure of CTAB (top) and a schematic representation of a micelle (bottom). CTA <sup>+</sup> has a non-polar carbon alkyl tail chain and a polar quaternary ammonium head group. Filled circles in the micelle represent head groups. . . . .	4
2.1	Regions and variables used in the solution of Poisson's equation. I and III are the interiors of the two polyelectrolytes, with dielectric constants $\epsilon_i$ , and fixed charges $e_j$ located at $\mathbf{r}_j$ . region II is the solvent with dielectric constant $\epsilon_w$ and charge density $\rho = -\kappa^2 \epsilon \Phi_2 / 4\pi$ . . . . .	16
2.2	Coordinates for the calculation. $\theta_j$ and $\phi_j$ are measured with respect to the line of centers. . . . .	17
2.3	Cross term $P_{0000}$ of the electrostatic interaction energy of two spheres, normalized relative to Phillies' analytic approximant, <sup>10</sup> Eq. (2.78). Here $\epsilon_w/\epsilon_i = 20$ and $r_1 = r_3 = a$ . At large $R$ and small $\kappa a$ , the analytic approximant becomes virtually exact. . . . .	37
2.4	Self term $P_{0000}^B$ of the electrostatic interaction energy of two spheres, normalized relative to Phillies' analytic approximant, <sup>10</sup> Eq. (2.78). Here $\epsilon_w/\epsilon_i = 20$ and $r_1 = r_3 = a$ . . . . .	38



- 
- 2.5 Cross term  $P_{0000}$  and self term  $P_{0000}^B$ , in units of  $k_B T$  for  $T = 298$ , for identical spherical polyelectrolytes with  $a = 25 \text{ \AA}$ ,  $Q_1 = Q_3 = 1$ , and  $\epsilon_w/\epsilon_i = 20$  at various ionic strengths. At small  $R$  and large  $\kappa a$ , the self-term dominates the better-known cross term; at large  $R$  and small  $\kappa a$  the cross term is dominant. . . . . 40
- 2.6 Cross term  $P_{0000}$  and self term  $P_{0000}^B$ , in units of  $k_B T$  for  $T = 298$ , for polyelectrolytes having radii  $r_1 = 25 \text{ \AA}$ ,  $r_3 = 350 \text{ \AA}$ , charges  $Q_1 = Q_3 = 1$ , and  $\epsilon_w/\epsilon_i = 20$  at various ionic strengths. At small  $R$  and large  $\kappa a$ , the self-term dominates the better-known cross term; at large  $R$  and small  $\kappa a$  the cross term is dominant. . . . . 41
- 2.7 The interaction energy at several ionic strengths for spherical polyelectrolytes of equal radius  $25 \text{ \AA}$  and opposite charge  $\pm 10e$ , in units of  $k_B T$  at  $298 \text{ K}$ . . . . . 42
- 2.8 Induced dipole (top) and counterion-exclusion effects (bottom). The dipole induced in each sphere by the charge of the other sphere causes the spheres to repel or attract each other depending on the ratio between dielectric constants of spheres and the solution. Exclusion of part of the counterion cloud of one sphere by the excluded volume of the other sphere is always unfavorable, contributing to sphere repulsion. 44
- 2.9 Self term  $P_{0000}^B$  of the interaction energy (in units of  $k_B T$  at  $298 \text{ K}$ ) for spherical polyelectrolytes of radius  $25 \text{ \AA}$  and unit charge, at several ionic strengths. Here  $\epsilon_w/\epsilon_i = 0.2$ ; for  $\epsilon_w/\epsilon_i < 1$ ,  $P_{0000}^B$  may be either attractive or repulsive. . . . . 45

2.10	Cross ( $P_{0000}$ ) and self ( $P_{0000}^B$ ) terms in the interaction energy at several ionic strengths for identical spherical polyelectrolytes of radius 25 Å and unit charge, in units of $k_B T$ at 298 K. Here $\epsilon_w/\epsilon_i = 1.0$ ; the dielectric constant discontinuity at the polyelectrolyte surfaces has been removed. In this system, $P_{0000}^B$ is due entirely to the exclusion of the counterion cloud by the other sphere. . . . .	47
2.11	Electrostatic interaction energies in units of $kT$ for spheres of unequal size, showing (a) cross and (b) self terms as functions of intersphere distance in reduced units. Spheres bear one electron charge and have radii $r_1$ and $r_3$ , with $\epsilon = 20$ , $I = 0.1\text{M}$ , and $T = 298\text{K}$ . . . . .	49
2.12	Electrostatic interaction energies in units of $kT$ for touching spheres of unequal size, showing (a) cross and (b) self terms as functions of sphere radii $r_1$ and $r_3$ . Spheres bear one electron charge; system has with $\epsilon = 20$ , $I = 0.1\text{M}$ , and $T = 298\text{K}$ . . . . .	50
3.1	Experimental setup for measuring mutual and probe diffusion coefficient with QELSS. . . . .	74
3.2	Interference of light scattered by two particles in a QELSS experiment. $\mathbf{k}_i$ is the wavevector of the incident light, $\mathbf{k}_s$ is the wavevector of the scattered light, and $\mathbf{Q} = \mathbf{k}_s - \mathbf{k}_i$ is the scattering vector. . . . .	76
3.3	Mutual diffusion coefficient $D_m$ of SDS micelles at temperature 35 °C against surfactant concentration $c$ at NaCl concentrations 0.1 M ( $\circ$ ), 0.2 M ( $\triangle$ ), 0.3 M ( $\square$ ), 0.4 M ( $\diamond$ ) and 0.5 M ( $\nabla$ ). Lines represent linear least-squares fits to $D_m$ and $D_p$ to obtain microscopic properties of micelles (see text). Data was taken by John Ren. <sup>1</sup> . . . . .	83

- 
- 3.4 Probe diffusion coefficient  $D_p$  of 67 nm polystyrene spheres in solutions of SDS:NaCl:H<sub>2</sub>O micelles at temperature 35 °C against SDS concentration  $c$  at NaCl concentrations 0.1 M ( $\circ$ ), 0.2 M ( $\triangle$ ), 0.3 M ( $\square$ ), 0.4 M ( $\diamond$ ) and 0.5 M ( $\nabla$ ). Lines represent linear least-squares fits to  $D_m$  and  $D_p$  to obtain microscopic properties of micelles (see text). Data was taken by Delphine Clomenil.<sup>1</sup> . . . . . 84
- 3.5 Mutual diffusion coefficient  $D_m$  of CTAB micelles at temperature 35 °C against surfactant concentration  $c$  at NaBr concentrations 0.01 M ( $\circ$ ), 0.05 M ( $\triangle$ ), 0.1 M ( $\square$ ), 0.2 M ( $\diamond$ ) and 0.3 M ( $\nabla$ ). Lines represent linear least-squares fits to  $D_m$  and  $D_p$  to obtain microscopic properties of micelles. Dashed parabola represents a quadratic fit to 0.01 M NaBr data to obtain the initial slope and intercept, as used in the fits (see text). Data was taken by the author.<sup>1</sup> . . . . . 86
- 3.6 Probe diffusion coefficient  $D_p$  of 240 nm polystyrene spheres in solutions of CTAB micelles in NaBr:H<sub>2</sub>O at temperature 35 °C against CTAB concentration  $c$  at NaBr concentrations 0.01 M ( $\circ$ ), 0.05 M ( $\triangle$ ), 0.1 M ( $\square$ ), 0.2 M ( $\diamond$ ) and 0.3 M ( $\nabla$ ). Lines represent linear least-squares fits to  $D_m$  and  $D_p$  to obtain microscopic properties of micelles (see text). Data was taken by the author.<sup>1</sup> . . . . . 87

## LIST OF TABLES

3.1	Analysis of SDS $D_m$ and $D_p$ data using my sphere-sphere electrostatic potential and eqs. (3.1) – (3.5) and (3.26) – (3.35). Asterisk indicates an inferred parameter. $I$ is the salt concentration, $a_m$ and $a_p$ are the micelle and probe radii, $q_m$ and $q_p$ are the corresponding charges (for all ionic strengths, $q_p=10000$ ), $a_c$ is the micellar radius of closest approach, $N_a$ is the micellar aggregation number, $h$ is the micellar hydration number in water molecules per surfactant molecule, $\delta$ is the micellar hydration in grams of water per gram of surfactant. $R_w$ is the equivalent water shell thickness, and $\bar{v}$ is the micellar partial volume.	95
3.2	Analysis of SDS $D_m$ and $D_p$ data using the Debye-Huckel potential and eqs. (3.1) – (3.5) and (3.26) – (3.35). Symbols are as in Table 3.1.	96
3.3	Analysis of CTAB $D_m$ and $D_p$ data, using my sphere-sphere electrostatic potential and eqs. (3.1) – (3.5) and (3.26) – (3.35). All symbols are as in Table 3.1. . . . .	97

- 
- 3.4 Analysis of SDS  $D_m$  and  $D_p$  data using my sphere–sphere electrostatic potential and micellar growth model described by Eq. (3.41).  $N_0$  and  $k_1$  are defined in Eq. (3.41),  $\alpha_m$  is the micellar fractional charge,  $a_m^0$  is the micellar radius at zero surfactant concentration. Columns 2–4 of the table summarize results of fits with  $k_1$  fixed at  $8.76 \text{ (g/mol)}^{-\frac{1}{4}}$ . In fits described by the last three columns  $k_1$  is a free parameter. . . . . 102

## 1. GENERAL INTRODUCTION

This thesis uses experimental and theoretical approaches to treat a problem of micelle diffusion in solutions. In the experimental part I measure the mutual diffusion coefficient of micelles and the diffusion coefficient of optical probes in a solution containing micelles using Quasi-Elastic Light Scattering Spectroscopy (QELSS). In the theoretical part I enhance and develop further the existing theory and use it to interpret the results of my experiment in terms of micellar microscopic parameters. This chapter briefly familiarizes the reader with terms used and problems treated in this thesis.

Micelles are aggregates of dissolved amphiphilic molecules. In an amphiphilic molecule one can point out spatially separated parts that exhibit substantially different solvation properties. Thus, an amphiphilic molecule in aqueous solution has a hydrophilic and a hydrophobic part. Thermal equilibration creates an effective force that aggregates amphiphilic molecules and orients them so that all hydrophobic molecular parts are inside the aggregate, whereas all hydrophilic molecular parts are facing outwards into the solvent (Figure 1.1).

A micelle is thought to have a defined closed shell shape, where the shell is formed by amphiphilic molecules aligned parallel to each other and perpendicular to the surface of the shell. Micelles are usually spherical or slightly elongated, but under certain conditions micelles can grow into very long worm-like entangled structures. The materials whose molecules form shells and layers in the same way molecules are

arranged in the micellar shell are called surfactants.

A micelle may be charged if the constituent amphiphilic molecules carry a charge or a dipolar moment. Micelles of cationic surfactants are positively charged and micelles of anionic surfactants are negatively charged. Charged micelles in solutions of electrolytes interact via a screened Coulomb potential, which is one of the foci of this thesis.

In a water–oil emulsion containing dissolved amphiphilic molecules, the micelles are formed around oil micro-droplets, coating the oil micro-droplets with a shell of surfactant. The amphiphilic molecules enhance wetting of the oil by essentially binding the oil droplets to the surrounding water. The property of binding oil to water makes amphiphilic molecules wonderful candidates for soap making. In fact, a molecule of the most popular commercial detergent, sodium lauryl sulfate, is the best example of an amphiphilic molecule. Sodium lauryl sulfate is an inexpensive detergent commonly used in cosmetic cleansers, hair shampoos, bath and shower gels, bubble baths, etc. (the ingredients of your favorite product in your bathroom). (Sodium lauryl sulfate is also probably the most potentially dangerous ingredient used in skin and hair-care products. Sodium lauryl sulfate is used in testing-labs as the standard skin irritant to compare the healing properties of other ingredients.)

In this thesis I study micelles of sodium dodecyl sulfate and cetyl trimethyl ammonium bromide surfactants. Sodium dodecyl sulfate (SDS,  $\text{NaC}_{12}\text{H}_{25}\text{SO}_4$ ) is a man-made form of the naturally occurring sodium lauryl sulfate. In aqueous solution an SDS molecule dissociates into a sodium and a dodecyl sulfate ( $\text{DS}^-$ ) ions. A  $\text{DS}^-$  ion consists of a non-polar alkyl chain of 12 carbon atoms, the “tail”, and a polar sulfate group, the “head”. SDS is amphiphilic because its polar head is hy-

drophilic and the non-polar tail is hydrophobic. SDS is an anionic surfactant, so SDS micelles are negatively charged. A molecule of cetyl trimethyl ammonium bromide (CTAB,  $C_{16}H_{33}(CH_3)_3NBr$ ) dissociates into a bromide and a cetyl trimethyl ammonium ( $CTA^+$ ) ion. A  $CTA^+$  ion consists of a non-polar sixteen carbon alkyl tail chain and a polar quaternary ammonium head group (Figure 1.1).  $CTA^+$  is a cation, so CTAB is a cationic surfactant, and CTAB micelles are positively charged.

From the measured micellar diffusion constant, I deduce the micellar radius, the micellar charge, and other micellar microscopic parameters. In addition to the dependence of the micellar diffusion coefficient  $D_m$  on the micellar radius and hydrodynamic drag coefficient,  $D_m$  depends on the micellar charge and the micellar concentration.  $D_m$  depends on the micellar charge because a QELLS experiment measures  $D_m$  as the average relaxation rate of micellar concentration gradients induced by thermal fluctuations. An increase in the micellar charge increases micellar repulsion, and therefore increases the relaxation rate of micellar concentration gradients. Also, in general,  $D_m$  is larger in more concentrated micellar systems, where micelles are in average closer to each other and repel each other stronger than in dilute micellar systems. However, if micelles attract each other,  $D_m$  may decrease with the micellar concentration.

I measured the dependence of  $D_m$  and  $D_p$  of CTAB in aqueous solutions with added NaBr on the CTAB concentration for several solution ionic strengths. John Ren and Delphine Clomenil measured  $D_m$  and  $D_p$  of SDS in NaCl:water as a function of SDS concentration. Analysis of the data using the old form for the electrostatic potential of two charged spheres  $q_1q_2 \exp[-\kappa(R - 2a)]/[\epsilon r(1 + \kappa a)^2]$  failed to produce consistent results. Using a novel mathematical treatment and a computer technique, I found a corrected form for the electrostatic interaction potential and an analytical



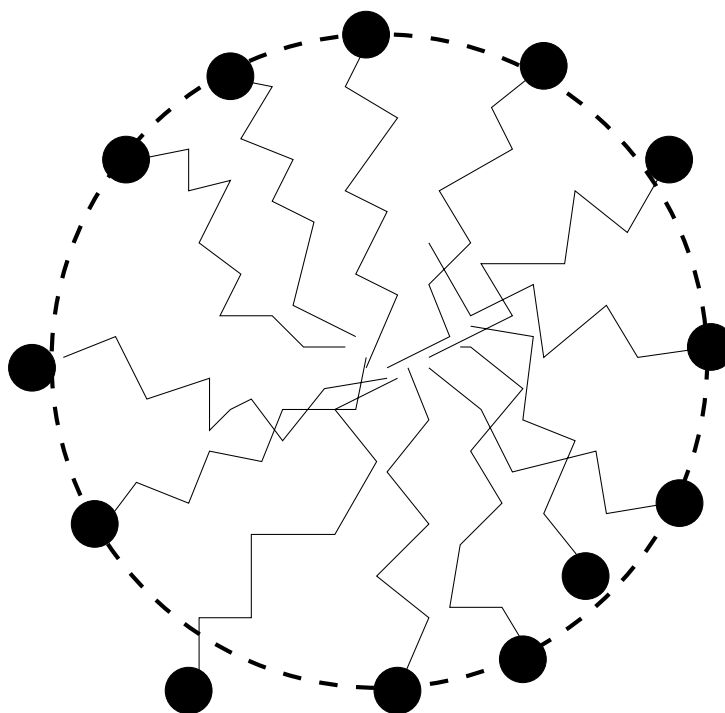
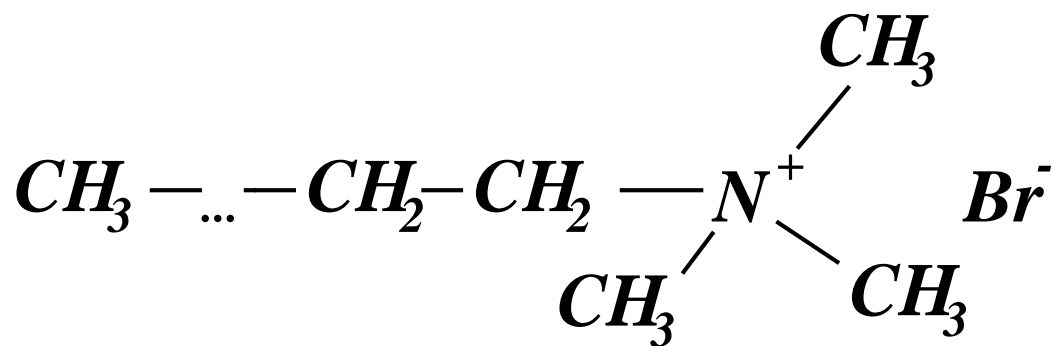


Fig. 1.1: Bond structure of CTAB (top) and a schematic representation of a micelle (bottom).  $\text{CTA}^+$  has a non-polar carbon alkyl tail chain and a polar quaternary ammonium head group. Filled circles in the micelle represent head groups.

form for a good approximation to the potential. Analysis of experimental data on CTAB and SDS using the correct form for the electrostatic interaction potential between micelles and between micelles and optical probes produced consistent micellar microscopic parameters.

The systems studied here, besides being interesting in their own right, are a model for a variety of fundamental and practical phenomena, such as self-organization of complex structures, intracellular diffusion in living cells, and enzymatic post-processing of polymers in biochemical engineering. Industrial applications of micelle-forming surfactants include detergents, cosmetics, drug delivery, environmental remediation, and enhanced oil recovery.

Developing an improved form for the sphere-sphere electrostatic interaction potential is very important for understanding of vesicle and cell-cell adhesion. Vesicles are closed-film structures which are being employed as simple containers to transport drugs within the blood system.

Improvements of the electrostatic interaction potential may help better understand the protein folding problem. All proteins have a certain energy associated with them, and it is the natural tendency to minimize this energy which causes a protein to fold as it does. Proteins are surrounded by an aqueous solution in the body, and this interaction with solvent as well as with itself helps to dictate how a protein folds. My work may be applied to correct the electrostatic interaction between two parts of a protein or between two proteins in the presence of screening solvent.

Simultaneous analysis of probe and mutual diffusion of charged micelles implemented here for the first time may be used to measure the anionic surfactant adsorption on environmental contaminants. The surfactant adsorption measurements are

necessary to identify and characterize surfactants suitable for environmental remediation applications.

Surfactant flooding is technically one of the most promising enhanced oil recovery processes. Surfactants make it easier for water to move oil droplets through a reservoir to producing wells. The surfactants act like detergents, breaking down the oil's resistance to the water and allowing the oil to be carried through the reservoir's tiny rock pores. The surfactant adsorption measurements are necessary to identify and characterize surfactants suitable for oil recovery applications.

Chapter 2 of this thesis derives the correct form for the electrostatic interaction potential of two charged spheres in a electrolyte solution. Chapter 3 studies diffusion of sodium dodecyl sulfate and cetyl trimethyl ammonium bromide micelles using QELLS and deduces microscopic parameters of micelles using results of Chapter 2. Chapter 4 gives concluding remarks and proposes future work. The Appendix gives the Mathematica code used to obtain the results of Chapter 2.

## 2. INTERACTION OF POLYELECTROLYTES

### 2.1 *Introduction*

The objective of this chapter is to treat the electrostatic interaction energy of a pair of charged dielectric spheres immersed in a screening medium. Physical systems realizing this model include charged micelles, proteins, and spherical colloids in aqueous electrolyte solutions. Electrostatic interactions of polyelectrolytes play an important role in a wide variety of physical problems, including solubility and salting-out effects,<sup>2,3</sup> protein titration,<sup>4</sup> the effect of substituents on organic acids' pK,<sup>5</sup> the stability of lyophobic colloids,<sup>6,7</sup> the excess chemical potential of polyelectrolyte solutions,<sup>8,10</sup> and the concentration dependence of the diffusion coefficient.<sup>11</sup>

My own interest in this problem arose from my studies of light scattering by micellar solutions of sodium dodecyl sulphate or cetyl trimethyl ammonium bromide. In these experiments, which are described in more detail in Chapter 3 of this thesis, I used quasi-elastic light scattering spectroscopy (QELSS) to determine the concentration dependence of the mutual diffusion coefficient  $D_m$  of the micelles; I also used QELSS to measure the single-particle diffusion coefficient  $D_p$  of polystyrene latex probes suspended in the micellar solutions. Efforts to interpret my measurements in terms of fundamental hydrodynamic theory<sup>12</sup> and a simple hard-sphere plus Debye-Hückel potential led to unsatisfactory values for micelle charge and aggregation num-

bers. A thorough examination of alternative explanations for the difficulty led me to improvements in the theory based the following calculations.

Section 2.2 of this chapter describes previous work on the subject of electrostatic interaction of ions in solution. Section 2.3 obtains the electrostatic interaction energy in the form of a spherical harmonic expansion with open-form expressions for the expansion coefficients. In Sec. 2.4, computer symbolic manipulation methods are used to find closed form approximations for the expansion coefficients. Finding the closed form requires truncation and inversion of an initially infinite matrix; in Sec. 2.4 the process is shown to be numerically convergent. Section 2.5 presents numerical evaluations of the closed-form terms using parameters appropriate to micelles in salt solution. Closing sections compare my findings with the literature and give conclusions. The work described here has been reported in the literature.<sup>1</sup>

## 2.2 Historical

In 1923 Debye and Hückel presented a linear theory<sup>13</sup> for the electrostatic potential created by a single macroion in an electrolyte. Their macroion charge distribution was spherically symmetric; all higher moments of the charge distribution vanished. For simple electrolyte producing ions of the valence types  $q_s$ , present at concentrations  $c_s$ , the potential in the region outside the macroion  $\phi(\mathbf{r})$  is described by Poisson-Boltzmann equation

$$\nabla^2 \phi(\mathbf{r}) = -\frac{4\pi}{\epsilon_w} \sum_s c_s q_s e^{-\beta q_s \phi(\mathbf{r})}, \quad (2.1)$$

where  $\epsilon_w$  is the dielectric constant of the solution,  $\beta = 1/k_B T$ ,  $k_B$  is the Boltzmann's constant, and  $T$  is the absolute temperature. With the electroneutrality condition

$$\sum_s c_s q_s = 0 \quad (2.2)$$

applied, linearization of the exponential gives the linear Poisson-Boltzmann equation:

$$\nabla^2 \phi(\mathbf{r}) = \kappa^2 \phi(\mathbf{r}), \quad (2.3)$$

where

$$\kappa^2 = \frac{4\pi\beta}{\epsilon_w} \sum_s q_s^2 c_s. \quad (2.4)$$

In the region inside the macroion the appropriate equation for  $\phi(\mathbf{r})$  is the Laplace equation

$$\nabla^2 \phi(\mathbf{r}) = 0. \quad (2.5)$$

Since the macroion is fixed at the origin and  $\phi(\mathbf{r})$  is spherically symmetric, it is convenient to use spherical coordinates. Equations 2.3 and 2.5 become

$$\frac{1}{r^2} \frac{\partial}{\partial r} \left( r^2 \frac{\partial \phi}{\partial r} \right) = \kappa^2 \phi(r), \quad (2.6)$$

and

$$\frac{1}{r^2} \frac{\partial}{\partial r} \left( r^2 \frac{\partial \phi}{\partial r} \right) = 0. \quad (2.7)$$

The spherically symmetric general solutions to these equations are

$$\begin{aligned}\phi(r) &= \frac{A_1 e^{-\kappa r}}{r} + \frac{B_1 e^{\kappa r}}{r}, \quad r > a \quad \text{and} \\ \phi(r) &= \frac{A_2}{r} + B_2 \quad 0 < r < a,\end{aligned}\tag{2.8}$$

where  $A_1, A_2, B_1,$  and  $B_2$  are constants of integration. The boundary conditions used to solve for unknown constants of integration in Eq. (2.8) are that  $\phi(\mathbf{r})$  must vanish as  $r \rightarrow \infty$  and that  $\phi(\mathbf{r})$  and  $\epsilon d\phi/dr$  must be continuous at the spherical surface of the macroion. The main result of the Debye–Hückel theory is the screened coulombic potential

$$\phi(\mathbf{r}) = \frac{q e^{-\kappa(r-a)}}{\epsilon r(1 + \kappa a)},\tag{2.9}$$

where  $q$  is the charge and  $a$  is the radius of the spherical macroion.

Kirkwood<sup>2</sup> extended the linear Debye–Hückel theory to account for the non-spherical charge distribution in the macroion. The macroion was allowed to have nonvanishing dipole, quadrupole, and higher multipole momenta of the charge distribution. The general solutions of eqs. 2.3 and 2.5 contained spherical harmonics of all orders. Using the same boundary conditions, Kirkwood obtained an expression for the electrostatic potential of the macroion at all points in space as a function of position and all multipole momenta of the macroion charge distribution.

Kirkwood<sup>3</sup> calculated the potential energy of dipolar ions of spherical and prolate ellipsoidal shapes. Kirkwood used the Laplace and linearized Poisson-Boltzmann equations (eqs. 2.3 and 2.5) to describe the electrostatic potential, but Kirkwood confined his treatment to limiting laws approached at high dilution and idealized

the solvent as a structureless dielectric continuum that does not cause electrostatic screening. Kirkwood neglected the terms small in the ratio of dielectric constants of the dipolar ion and the solution,  $\epsilon_i/\epsilon_w$ . In his treatment of non-spherical dipolar ions Kirkwood included the “salting-out” forces between an ion in solution and a dipolar ion. The “salting-out” forces represent a repulsion between a real ion and its image charge distribution in the cavity occupied by the dipolar ion in the solvent. Kirkwood claimed that a similar effect arising from the interaction of the dipolar ion and an image distribution in the ionic cavity was usually of much smaller magnitude and could be neglected.

Kirkwood and Shumaker<sup>8</sup> extended the linear Debye–Hückel theory to include interactions between pairs of macroions. The macroions were allowed to have non-vanishing charge multipole moments. Kirkwood and Shumaker computed terms in the excess chemical potential of the polyelectrolytes arising from fluctuations in the net polyelectrolyte charge. The potential of average force between two ions  $W(r)$  was calculated by averaging the potential  $V(R)$  of the force in fixed orientation and charge configuration of the ions as

$$\begin{aligned} \exp(-\beta W(R)) &= \langle \exp(-\beta V) \rangle_{Av} \\ W(R) &= \langle V(R) \rangle_{Av} - \frac{\beta}{2} [\langle V^2 \rangle_{Av} - \langle V \rangle_{Av}^2] + O(\beta^2), \\ V(R) &= \sum_{i,k} \frac{q_i q_k}{\epsilon_w R_{ik}} \end{aligned} \quad (2.10)$$

where  $R_{ik}$  is the scalar distance between charge group  $i$  of macroion 1 and charge group  $k$  of the macroion 2,  $q_i$  and  $q_k$  are the charges of the respective groups, and the average was taken over all orientations and over all charge configurations of the two



macroions, with uncorrelated distribution functions.

The potential  $W(R)$  leads Kirkwood and Shumaker to a long-range attractive force diminishing as the inverse cube of the distance between the two macroions in the absence of screening. A force of this range fails to yield convergent expressions for the thermodynamic functions. For spherical macroions Kirkwood and Shumaker included a Debye–Hückel factor for screening of this electrostatic interaction of the form

$$W'(R) = W(R) \frac{e^{-2\kappa(R-a_{12})}}{(1 + \kappa a_{12})^2}, \quad (2.11)$$

where  $a_{12}$  is the sum of the radii of the two macroions.

Bahe<sup>9</sup> suggested that the effect of a point charge on water is to polarize the water locally, reducing the local dielectric constant from 80 to approximately 4. Bahe calculated the interaction of the gradient of the dielectric constant near the surface of an ion immersed in water, with the electric field generated by another ion. In Bahe's model the ion is an incompressible sphere with a charge located at the center; and water is a continuous dielectric medium with the properties of liquid water and the dielectric constant described by a piecewise linear function of distance from the center of the ion. For an ion with radius 1.5 Å Bahe assumed that the dielectric constant of water increases linearly from 3 to 81 as the distance from the center increases from 1.5 to 4.5 Å. The dielectric constant of water is 81 for distances larger than 4.5 Å. Bahe calculated the volume force vector  $\vec{F}$  acting on a region of space in a dielectric

as

$$\vec{F} = \rho \vec{E} - \frac{\epsilon_0}{2} E^2 \vec{\nabla} k + \frac{\epsilon_0}{2} \vec{\nabla} \left( E^2 \frac{dk}{dg} g \right), \quad (2.12)$$

where  $\rho$  is the charge density,  $\vec{E}$  is the electric field,  $k$  is the dielectric constant, and  $g$  is the mass density. Bahe obtained the energy of two ions by integrating the combination of the Coulomb force and the volume force given by Eq. (2.12) from  $\infty$  (zero point of electric energy) to  $R$ . The resultant electrostatic energy of two ions is

$$E = \frac{q_+ q_-}{k} \frac{1}{R} + \frac{\epsilon_0}{4} \frac{q_+^2}{k_0^2} \left| \frac{dk}{dR} V_{\text{sea}} \frac{1}{R^3} \right|, \quad (2.13)$$

where  $q_+$  and  $q_-$  are the ion charges,  $k_0$  is the dielectric constant at the surface of the ion, and  $V_{\text{sea}}$  is the volume of gradient sea around the ion.

Phillies<sup>10</sup> has extended the results of Kirkwood<sup>8</sup> by allowing the macroions to have dipole and quadrupole moments. His approach<sup>10</sup> was to solve the Debye-Hückel model numerically, obtaining the interaction energy of charges, dipoles, and quadrupoles, and then to find simple analytic approximations for these interactions. The resultant simplified electrostatic interaction potential was of the form

$$\begin{aligned} V(R) = & \frac{Q_1 Q_2}{\epsilon_w} \frac{e^{-\kappa R}}{R} C_0^2 + \frac{2Q_1 D_2 \cos \theta_2}{\epsilon_w} \frac{e^{-\kappa R} (1 + \kappa R)}{R^2} C_0 C_1 + \\ & \frac{D_1 D_2}{\epsilon_w} \cos \theta_1 \cos \theta_2 \frac{e^{-\kappa R} [2 + 2\kappa R + (\kappa R)^2]}{R^3} C_1^2 + \\ & \frac{D_1 D_2}{\epsilon_w} \sin \theta_1 \sin \theta_2 \cos(\phi_2 - \phi_1) \frac{e^{-\kappa R} (1 + \kappa R)}{R^3} C_1^2, \end{aligned} \quad (2.14)$$

where  $Q$  is the net charge of an ion,  $D$  is the magnitude of its dipole moment (which is taken to lie along the orientation vector), the subscripts 1 and 2 distinguish between

variables associated with different ions,  $\epsilon_w$  is the dielectric constant of the solvent,  $\epsilon_i$  is the dielectric constant inside the ions,  $\epsilon = \epsilon_w/\epsilon_i$ ,  $a$  is the radius of both ions, and where

$$\begin{aligned} C_0 &= \frac{e^{\kappa a}}{1 + \kappa a} \\ C_1 &= \frac{3e^{\kappa a}}{[2 + 2\kappa a + (\kappa a)^2 + (1 + \kappa a)/\epsilon]}. \end{aligned} \quad (2.15)$$

Phillies<sup>10</sup> also calculated the excess chemical potential arising from fluctuation of charges  $Q_1$  and  $Q_2$  and dipole moments  $D_1$  and  $D_2$ .

Here I will show that recent developments in spherical harmonic expansions<sup>14</sup> and computer symbolic manipulation techniques permit a purely analytic determination of the expressions that Ref. 10 obtained numerically. I will present open-form expressions and closed-form approximations for the electrostatic interactions between two spherical polyelectrolytes of unequal radii. In addition to the long range charge–charge term

$$V(R) = \frac{Q^2}{\epsilon_w R} \frac{\exp[-\kappa(R - 2a)]}{(1 + \kappa a)^2} \quad (2.16)$$

of Verwey and Overbeek,<sup>7</sup> I obtain shorter-range charge-induced dipole terms often overlooked. (Here  $Q$  and  $a$  are the colloid charge and radius, and  $\epsilon_w$  and  $\kappa$  are the solvent dielectric constant and inverse Debye length, respectively, while  $R$  is the center-to-center distance.) To anticipate my most important result, at short but physically interesting distances, with parameters appropriate to ionic micelles, charge-induced dipole terms dominate the charge–charge term of eq. 2.16.

Fisher *et al.*<sup>24–26</sup> studied approximately the same problem. Fisher *et al.* preceded

me in identifying the importance of the charge-induced dipole ( $q_1^2, q_2^2$ ) terms for the electrostatic interaction of two non-pointlike charged spheres. My results differ from those of Fisher *et al.* in that they obtained at intermediate stages series expansions in  $\kappa a$  and  $\exp(-\kappa R)/R$  which they truncated at low order in each variable. In contrast, I retained all terms of higher order in both  $\exp(-\kappa R)/R$  and  $\kappa a$ .

### 2.3 Electrostatic Interactions — General Results

In this section I calculate the electrostatic interaction energy  $U(R)$  of a pair of polyelectrolytes in a solution containing a simple electrolyte. The complete model (Fig. 2.1) contains two dielectric spheres 1 and 2 having radii  $r_1$  and  $r_2$ , center-to-center distance  $R$ , and dielectric constant  $\epsilon_i$ . Each sphere contains fixed charges  $e_j$  at locations  $\mathbf{r}_j$ , with  $j \in (1, N)$  for the first sphere and  $j \in (1, M)$  for the second sphere. The spheres divide space into three regions, namely region I within the first sphere, region II in the intervening space, and region III within the second sphere. The solvent, which contains a simple electrolyte, has dielectric constant  $\epsilon_w$ . It is convenient to define  $\epsilon = \epsilon_w/\epsilon_i$ . The local charge density in the solvent (region II) is induced by the fixed charges on the two polyelectrolytes, and is assumed to be given by the linearized Poisson–Boltzmann equation. From this equation, the charge density  $\rho(\mathbf{r})$  in region II is

$$\rho(\mathbf{r}) = -\frac{\kappa^2 \Phi_2 \epsilon_w}{4\pi} \quad (2.17)$$

where in cgs units

$$\kappa^2 = \frac{8\pi N e^2 I}{1000 \epsilon_w k_B T}. \quad (2.18)$$

Here  $\kappa$  is the Debye–Hückel inverse screening length,  $e$  is the electron charge,  $N$  is Avogadro’s number,  $I$  is the molar ionic strength of the solvent,  $T$  is the absolute temperature,  $k_B$  is Boltzmann’s constant, 1000 converts moles/liter to moles  $\text{cm}^{-3}$ , and  $\Phi_2(\mathbf{r})$  is the electrostatic potential at  $\mathbf{r}$ .

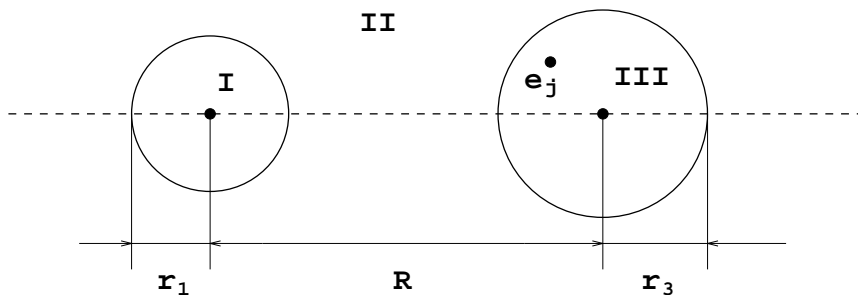


Fig. 2.1: Regions and variables used in the solution of Poisson’s equation. I and III are the interiors of the two polyelectrolytes, with dielectric constants  $\epsilon_i$ , and fixed charges  $e_j$  located at  $\mathbf{r}_j$ . region II is the solvent with dielectric constant  $\epsilon_w$  and charge density  $\rho = -\kappa^2 \epsilon \Phi_2 / 4\pi$ .

Figure 2.2 shows the (spherical polar) coordinates used in these calculations. Coordinates are  $\mathbf{r} = (r, \theta, \phi)$  centered on sphere 1 and  $\mathbf{r}' = (r', \theta', \phi')$  centered on sphere 2. If  $\mathbf{r}$  and  $\mathbf{r}'$  refer to the same point,  $\phi = \phi'$ . The conventions are the same as in Phillies,<sup>10</sup> except that  $\theta$  and  $\theta'$  are measured from the line of centers of the spheres in the same direction, rather than in opposite directions as in Ref. 10.

I now solve Poisson’s equation (in regions I and III) and the linearized Poisson–Boltzmann equation (in region II) to compute the electrostatic potential  $\Phi$  in each region. A charging process gives the interaction energy of the two spheres. The

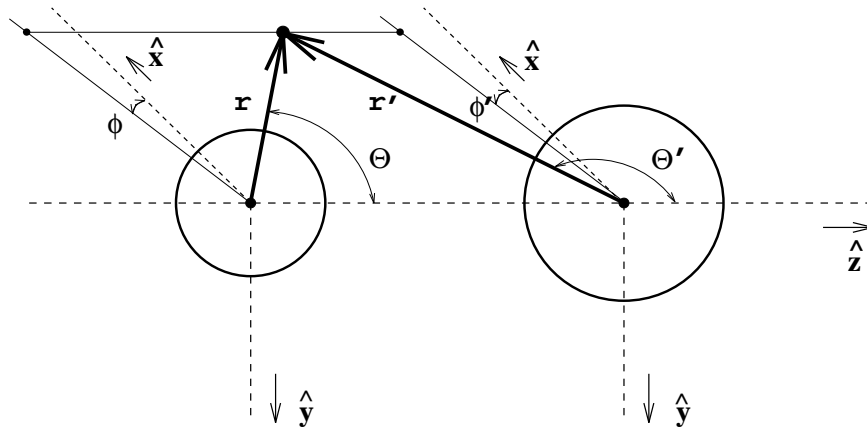


Fig. 2.2: Coordinates for the calculation.  $\theta_j$  and  $\phi_j$  are measured with respect to the line of centers.

underlying differential equations for  $\Phi$  are linear, so the electrostatic potential arising from the fixed charges in each sphere can legitimately be calculated while neglecting the contributions to the potential created by the fixed charges in the other sphere. If the linearized Poisson–Boltzmann equation were replaced with its correct nonlinear generalization, this neglect would no longer be justifiable.

$\Phi$  and the specified fixed charges in the two spheres are finally used to calculate  $U(R)$ .  $U(R)$  contains four terms. Two terms refer to the interaction of the fixed charges within each sphere with the electrostatic potential created within that sphere by the fixed charges in the other sphere. I call these terms the cross terms of  $U(R)$ . These terms vanish as  $R \rightarrow \infty$ . The other two terms refer to the interaction of the fixed charges in each sphere with the electrostatic potential those charges induce in their own sphere. I call these terms the self terms of  $U(R)$ . The self terms include interactions between charges within each sphere, ions in the surrounding solvent, and the induced polarization and excluded volume of the other sphere. The self terms depend on  $R$ , but do not vanish as  $R \rightarrow \infty$ .

The model is symmetric under exchange of labels between spheres 1 and 2, and regions I and III. It is therefore necessary to calculate explicitly only the self and cross terms created by the fixed charges in one of the two spheres. The self and cross terms arising from the charges in the other sphere may be obtained by symmetry on the labels. I now obtain the terms arising from the fixed charges in region I. The potential  $\Phi_j$  induced in region  $j$  by these fixed charges follows from

$$\nabla^2 \Phi_1(\mathbf{r}) = -\frac{4\pi}{\epsilon_i} \sum_{j=1}^N e_j \delta(\mathbf{r} - \mathbf{r}_j), \quad (2.19)$$

$$\nabla^2 \Phi_2 = \kappa^2 \Phi_2, \quad (2.20)$$

and

$$\nabla^2 \Phi_3 = 0. \quad (2.21)$$

The Poisson and Poisson–Boltzmann equations are solved by expanding the charge distribution and potential in each region in terms of spherical harmonics and appropriate radial functions. The expansion coefficients are determined by the boundary conditions and the fixed charges. In regions I and III,  $\Phi$  can be written in terms of spherical harmonics  $Y_{lm}(\theta, \phi)$  or  $Y_{lm}(\theta', \phi')$ , and powers of  $r$  or  $r'$ , respectively, namely

$$\Phi_1 = \sum_{l=0}^{\infty} \sum_{m=-l}^l (A_{lm} r^{-(l+1)} + B_{lm} r^l) Y_{lm}(\theta, \phi), \quad (2.22)$$

and

$$\Phi_3 = \sum_{l=0}^{\infty} \sum_{m=-l}^l (J_{lm} (r')^l + K_{lm} (r')^{-(l+1)}) Y_{lm}(\theta', \phi'). \quad (2.23)$$

In region II, the potential is determined by Eq. (2.20) and the requirement that the potential should go to zero at large  $r$ . Kirkwood<sup>2</sup> has shown that a complete set



of solutions for Eq. 2.20 that satisfy the condition  $\Phi \rightarrow 0$  as  $r \rightarrow \infty$  is

$$\Phi = \sum_{l=0}^{\infty} \sum_{m=-l}^l \frac{C_{lm} e^{-\kappa r}}{r^{l+1}} K_l(\kappa r) Y(\theta, \phi), \quad (2.24)$$

where  $K_l(\kappa r)$  is the  $l$ th-order polynomial part of the solution to the radial part of Eq. (2.20). The  $K_l(\kappa r)$  are explicitly given by

$$K_l(\kappa r) = \sum_{s=0}^l \frac{2^s l! (2l-s)!}{(2l)!(l-s)!} (\kappa r)^s. \quad (2.25)$$

Kirkwood's solution [Eq. 2.24] is equally valid for coordinates centered on either sphere. For my problem, a complete solution to eq. 2.20 is usefully written as the sum of two complete sets of these solutions, one centered on each sphere, namely

$$\Phi_2 = \sum_{l=0}^{\infty} \sum_{m=-l}^l \left( \frac{E_{lm} e^{-\kappa r} K_l(\kappa r)}{r^{l+1}} Y_{lm}(\theta, \phi) + \frac{F_{lm} e^{-\kappa r'} K_l(\kappa r')}{(r')^{l+1}} Y_{lm}(\theta', \phi') \right). \quad (2.26)$$

The potential and the perpendicular component of the electric field satisfy boundary conditions that determine relations between the expansion coefficients and the fixed charges. At the  $j - k$  boundary, these conditions are

$$\Phi_j = \Phi_k \quad (2.27)$$

and

$$\epsilon_j \frac{\partial \Phi_j}{\partial \hat{r}} = \epsilon_k \frac{\partial \Phi_k}{\partial \hat{r}}, \quad (2.28)$$

where  $\hat{r}$  is the normal to the boundary,  $\epsilon_j$  is the dielectric constant in region  $j$  and  $\Phi_j$  is the electrostatic potential in region  $j$ .

In order to use the boundary conditions to solve for the  $B_{lm}$ ,  $E_{lm}$ ,  $F_{lm}$ , and  $J_{lm}$ , it is highly convenient to be able to write  $\Phi_2$  on the surface of either sphere entirely in terms of spherical harmonics centered on a single sphere. To do this, functions  $f(r)Y_{lm}(\theta, \phi)$  centered on sphere 1 must be expanded in terms of functions  $f'(r')Y_{l'm'}(\theta', \phi')$  centered on sphere 2, and vice versa. A general procedure for obtaining the needed expansion was obtained by Silverstone and Moats,<sup>14</sup> who showed how to express a function  $F(\mathbf{r}) = f(r)Y_{LM}(\theta, \phi)$  in terms of spherical harmonics and radial functions centered on a new origin displaced from  $\mathbf{r} = 0$  by  $\mathbf{R} = (R, \theta_R, \phi_R)$ . From Ref. 14,  $F(\mathbf{r})$  may be expanded as

$$F(\mathbf{r} - \mathbf{R}) = \sum_{\substack{l=0 \\ l+L+\lambda \text{ even}}}^{\infty} \sum_{\lambda=|l-L|}^{l+L} \nu_{l\lambda L}(r, R) \sum_{m=-l}^l C_{\lambda LMlm} Y_{\lambda, M-m}(\theta_R, \phi_R) Y_{lm}(\theta, \phi) \quad (2.29)$$

where

$$C_{\lambda LMlm} = \int d\Omega Y_{\lambda, M-m}^*(\theta, \phi) Y_{lm}^*(\theta, \phi) Y_{LM}(\theta, \phi), \quad (2.30)$$

$$\nu_{l\lambda L}(r, R) = \frac{2\pi(-1)^l}{R} \sum_{a=0}^{(L+l+\lambda)/2} \sum_{b=0}^{(L+l+\lambda-2a)/2} D_{l\lambda Lab} \left(\frac{r}{R}\right)^{2b-l-1} \int_{|r-R|}^{r+R} \left(\frac{r'}{R}\right)^{2a-L+1} f(r') dr', \quad (2.31)$$

$$D_{l\lambda Lab} = 1/[(2a)!!(2a - 2L - 1)!!(2b - 2l - 1)!!(L + l + \lambda - 2a - 2b)!! \\ \times (2b)!!(L + l - \lambda - 2a - 2b - 1)!!], \quad (2.32)$$

$$(2N)!! = 2^N N!, \quad (2.33)$$

$$(2N - 1)!! = (2N)!/(2N)!!, \quad (2.34)$$

and

$$(-2N - 1)!! = (-1)^N/(2N - 1)!! \quad (2.35)$$

Here  $d\Omega = d\theta d\phi \sin(\theta)$ , while  $\theta_R$  and  $\phi_R$  are the angular components of the vector  $\mathbf{R}$ . The  $Y_{lm}(\theta, \phi)$  follow the normalization of Edmonds,<sup>15</sup> so  $Y_{lm}^*(\theta, \phi) = (-1)^m Y_{l,-m}(\theta, \phi)$ .

I now solve general forms of the electrostatic potential in Regions I, II, and III (eqs. 2.22, 2.26, and 2.23) and boundary conditions at boundaries of the Regions I – II and II – III (eqs. 2.27 and 2.28) for integration constants  $A_{lm}$ ,  $B_{lm}$ , and  $J_{lm}$ . The constants  $A_{lm}$  are determined by the fixed charges within region I. Solution of Eq. (2.19) combined with Eq. (2.22) gives

$$A_{lm} = \sum_{j=1}^n \frac{e_j (r_j)^l}{\epsilon_i} Y_{lm}^*(\theta_j, \phi_j) \frac{4\pi}{2l + 1}. \quad (2.36)$$

Since I am computing the part of  $\Phi$  due to the charges in region I, the potential is nonsingular in region III;  $K_{lm} = 0$  for all  $l$  and  $m$ .

Using the Silverstone–Moats expansion, the term of Eq. (2.26) containing  $F_{lm}$